# Supporting Information

Temperature and Length-Dependent Defect Photoluminescence in Biocompatible Cross-Linked Polymer-Coated Locally Functionalized Single-Walled Carbon Nanotubes

Ryo Hamano[1], Yoshiaki Niidome[1], Naoki Tanaka[1,2], Tomohiro Shiraki[1,2], Tsuyohiko Fujigaya*[,1, 2, 3]

[1] *Department of Applied Chemistry, Graduate School of Engineering, Kyushu University, 744 Motooka, Fukuoka 819-0395, Japan*
[2] *International Institute for Carbon Neutral Energy Research (WPI I²CNER), Kyushu University, 744 Motooka, Fukuoka 819-0395, Japan*
[3] *Center for Molecular Systems (CMS), Kyushu University, 744 Motooka, Fukuoka 819-0395, Japan*

**Table S1.** The estimated SWCNT concentration of length sorted gel-coated lf-SWCNTs-*p*$NO_2$ and gel-coated lf-SWCNTs-*o*P

| Sample | SWCNT concentration [ nM] | | | | |
|---|---|---|---|---|---|
| | Unsorted (injection) | fr1 | fr2 | fr3 | fr4 |
| Gel-coated lf-SWCNTs -*p*$NO_2$ | 5.65 | 0.048 | 0.096 | 0.637 | 0.397 |
| Gel-coated lf-SWCNTs -*o*P | 6.82 | 0.086 | 0.193 | 0.133 | 0.071 |

**Table S2**. Calculated $\Delta E_{optical}$, $\Delta E_{thermal}$, and $\lambda$ values of $E_{11}^*$ PL of unsorted and length sorted gel-coated lf-SWCNT-*o*P in $H_2O$.

| Sample | Average SWCNT length [nm] | $\Delta E_{optical}$ [meV] | $\Delta E_{thermal}$ [meV] | $\lambda$ [meV] |
|---|---|---|---|---|
| Unsorted | 231.9 | 143 | 51 | 92 |
| Fr1 | 367.1 | 139 | 51 | 88 |
| Fr2 | 245.1 | 140 | 50 | 90 |
| Fr3 | 164.3 | 143 | 53 | 90 |
| Fr4 | 117.6 | 145 | 20 | 126 |

To calculated the integrated intensity, PL peaks were deconvoluted based on the Voigt function and the peak area was estimated using package Multi peak fitting in Igor Pro (ver. 6.36J).

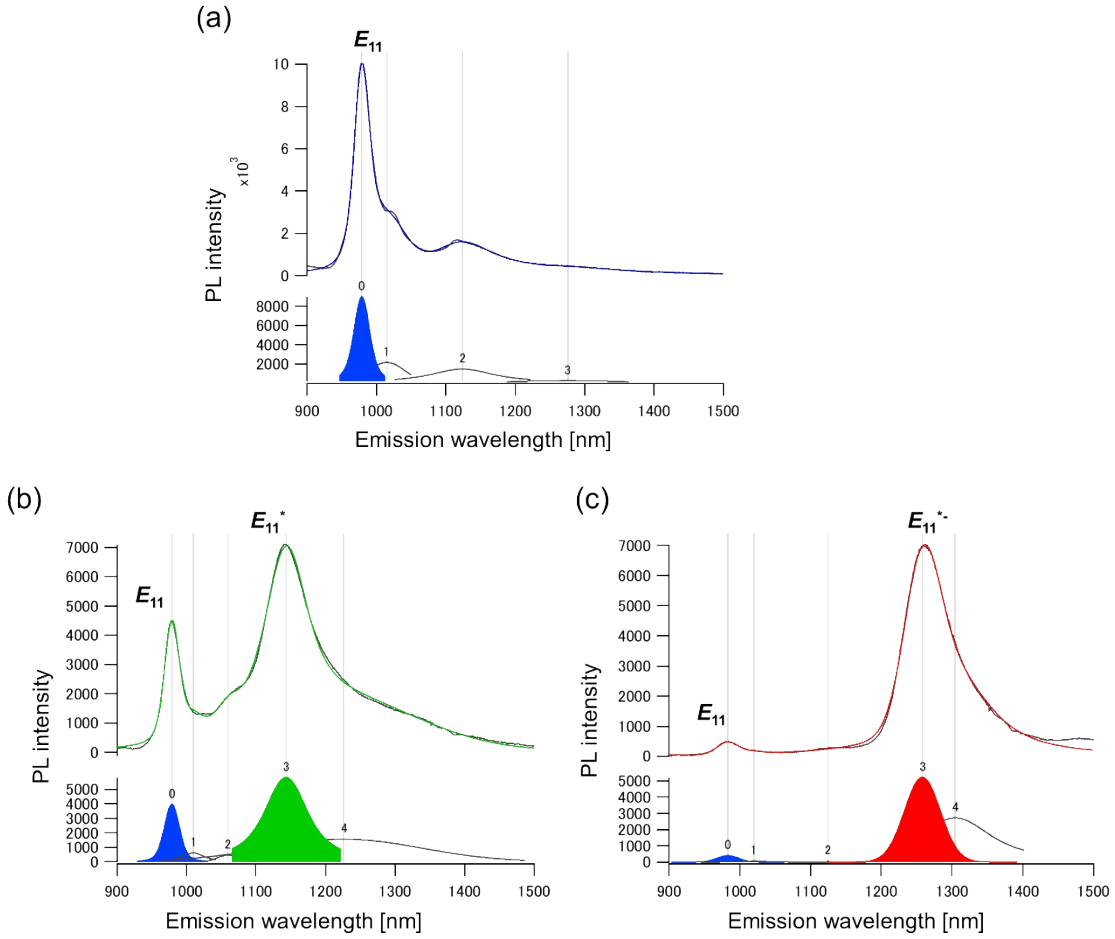


**Fig. S1** Deconvoluted PL spectra of (a) SDBS-dispersed SWCNTs, (b)SDBS-dispersed lf-SWCNTs-*p*$NO_2$, and (c) SDS-dispersed lf-SWCNTs-*o*P in $D_2O$.

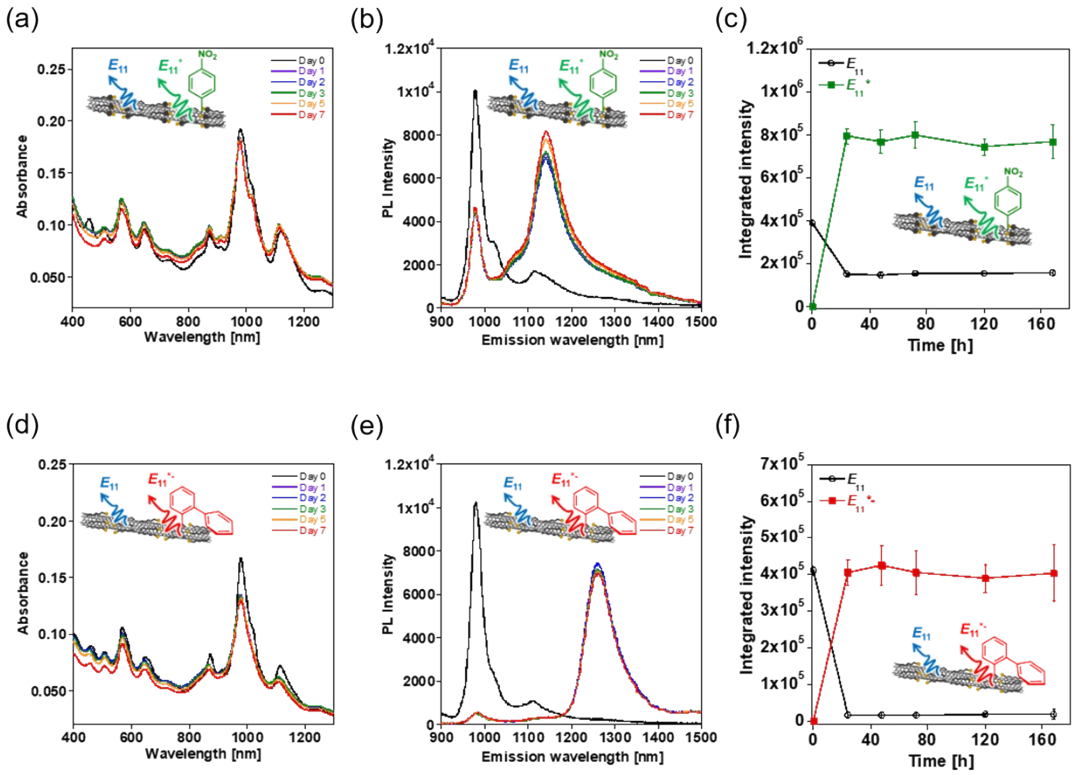


**Fig. S2** Time course (a) absorption spectra, (b) PL spectra (excitation: 570 nm) and (c) integrated $E_{11}$ and $E_{11}^{*}$ PL intensity of SDBS-dispersed lf-SWCNTs-*p*$NO_2$ in $D_2O$ monitoring for 7 days. The final concentration of Dz-*p*$NO_2$ [Dz-*p*$NO_2$] was 25.6 µM. Time course (d) absorption spectra, (e) PL spectra (excitation: 570 nm) and (f) integrated $E_{11}$ and $E_{11}^{*-}$ PL intensity of SDS-dispersed lf-SWCNTs-*o*P in $D_2O$. The final concentration of Dz-*o*P [Dz-*o*P] was 6.4 µM. The spectra before the addition of the diazonium salts were also displayed as Day 0 (black line). Error bars mean the error estimated during peak deconvolution.

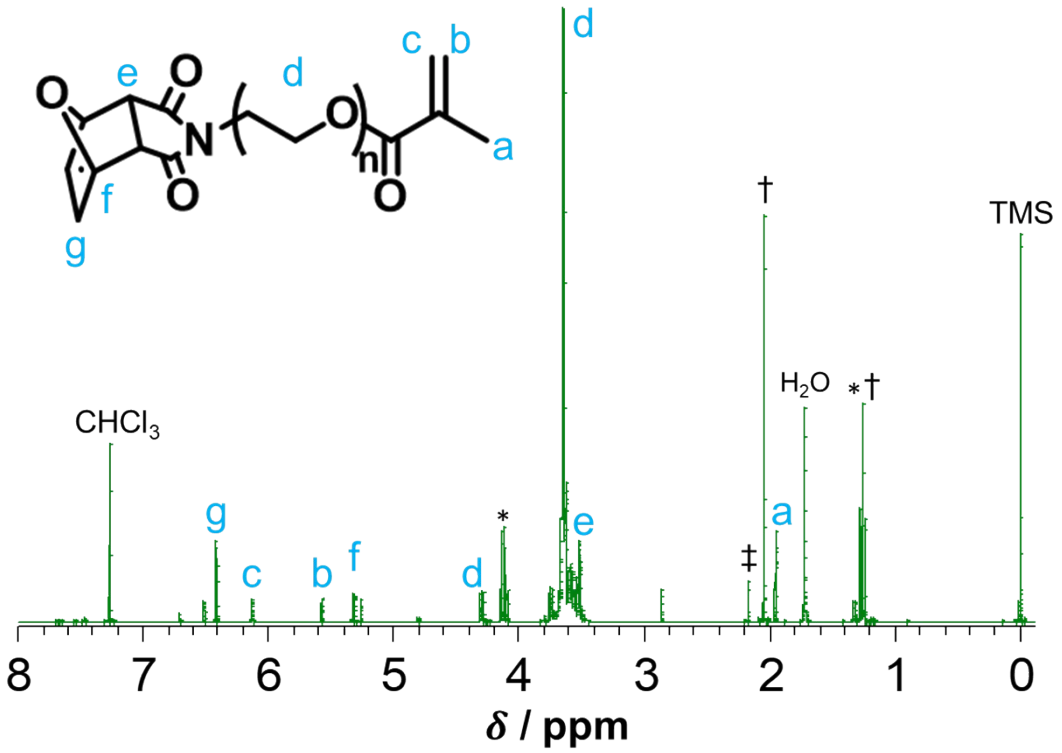


**Fig. S3** $^{1}$H NMR spectra of *endo*-FpMMA. Peaks indicated as *, †and ‡ can be assigned to the peaks of solvents (diethyl acetate, ethyl acetate and toluene, respectively) used for starting material and column purification.

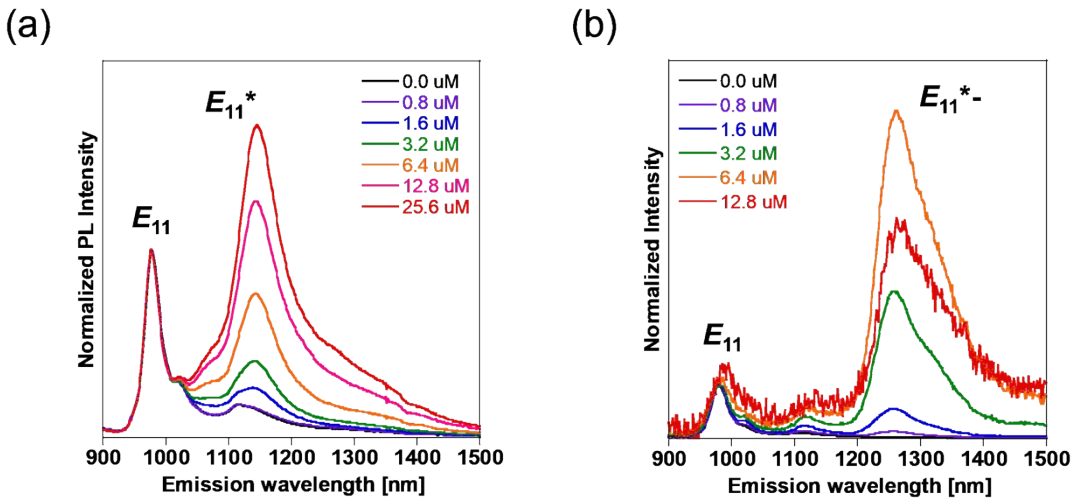


**Fig. S4** Normalized PL spectra (excitation: 570 nm) of (a) lf-SWCNTs-*p*$NO_2$ in SDBS solution and (b) lf-SWCNTs-*o*P in SDS solution react with different [Dz-*p*$NO_2$] and [Dz-*o*P], respectively.

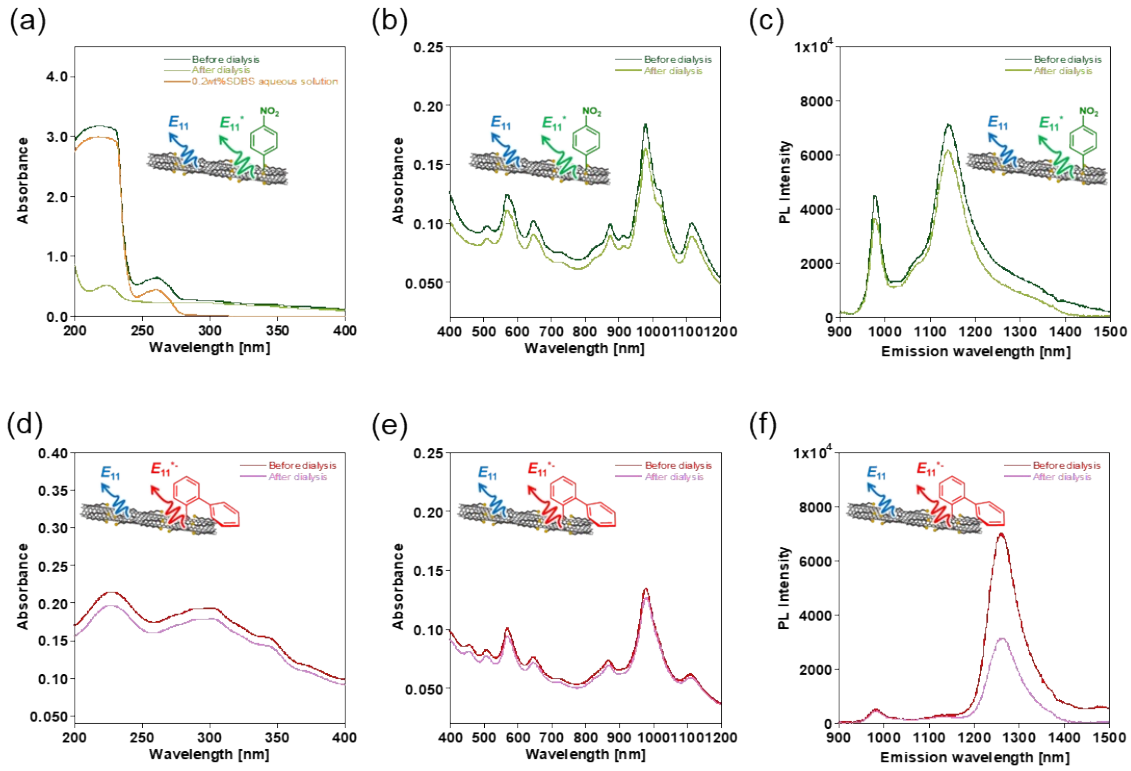


**Fig. S5** (a, b) The absorption and (c) PL spectra (excitation: 570 nm) of lf-SWCNTs-*p*$NO_2$ before (green) and after (light green) dialysis. The absorption spectrum of the aqueous SDBS solution was also displayed as reference (orange). (d, e) The absorption and (f) PL spectra (excitation: 570 nm) of lf-SWCNTs-*o*P before (red) and after (pink) dialysis.

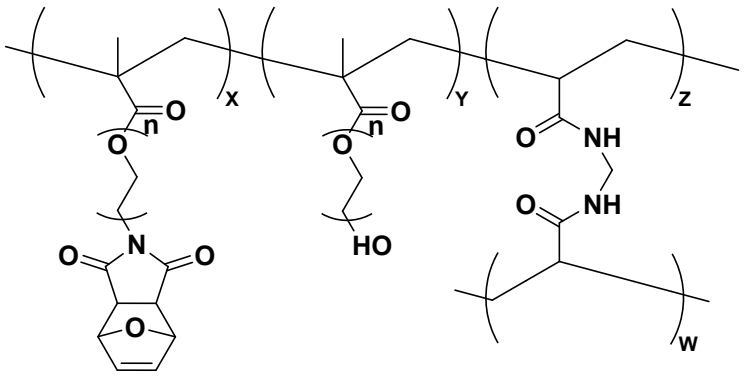


**Fig S6**. Chemical structure of the gel in *endo*-FpM/PEG.

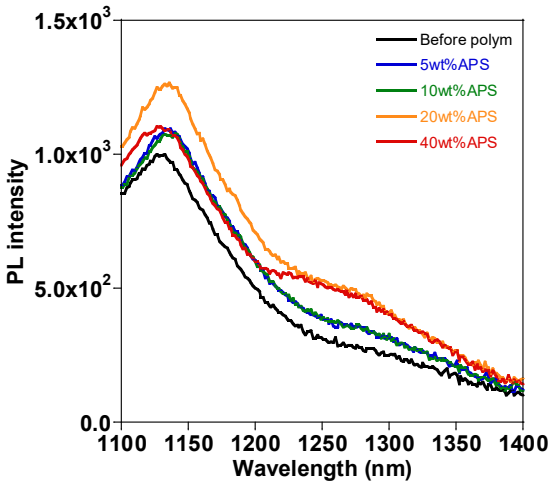


**Fig. S7** PL spectra (excitation: 570 nm) of SDS-dispersed SWCNT after CNT micelle polymerization using different concentration of APS, where PEGAM and *endo*-FpMMA were used as monomer.

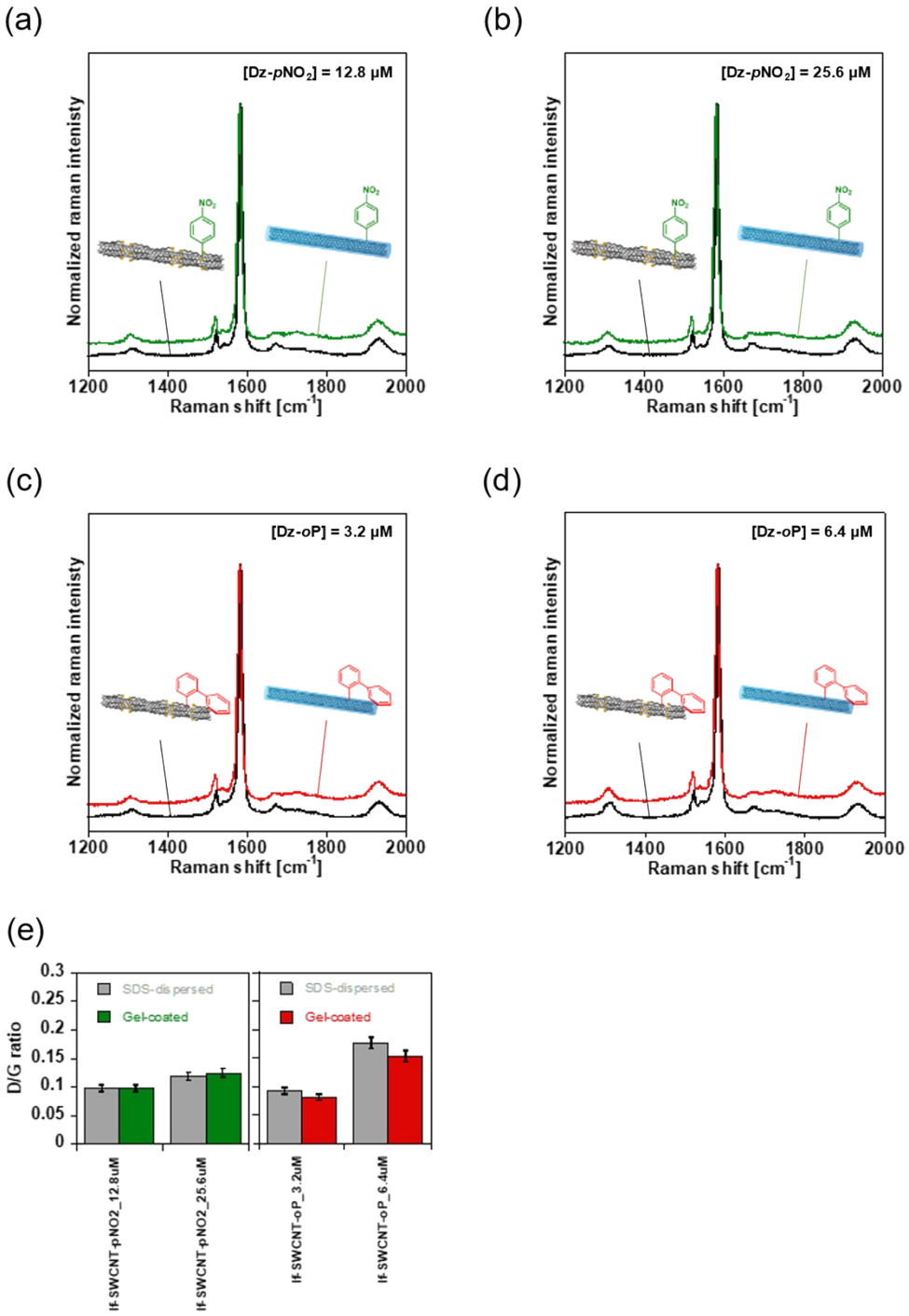


**Fig. S8** Normalized Raman spectra of (a, b) lf-SWCNTs-*p*$NO_2$ and (c, d) lf-SWCNTs-*o*P before (black) and after CNT micelle polymerization. (e) D/G ratio of lf-SWCNTs-*p*$NO_2$ (left panel) and lf-SWCNTs-*o*P (right panel) before and after the polymerization. Error bars mean the error estimated during peak deconvolution.

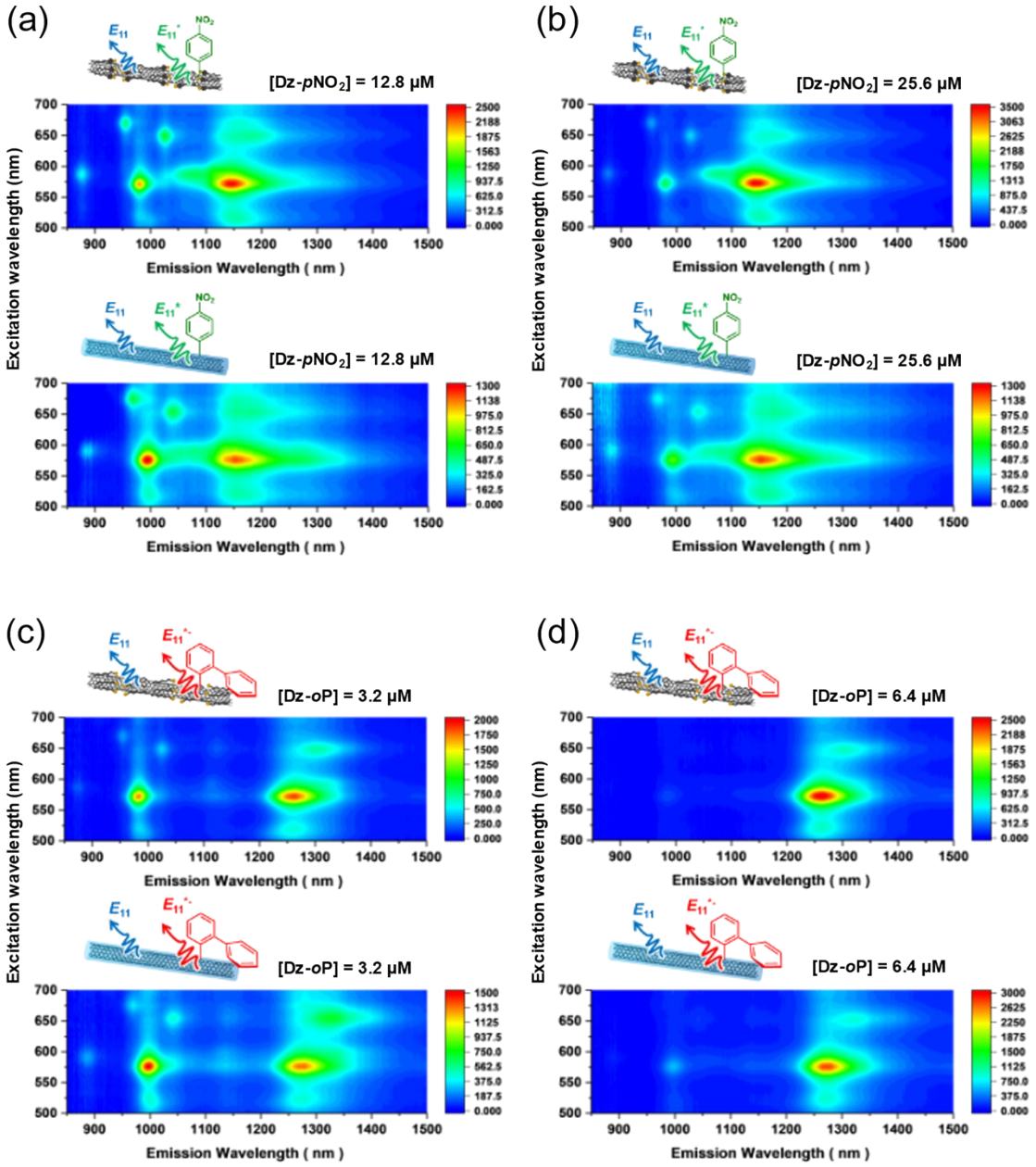


**Fig. S9** PL contour plot of (a) lf-SWCNTs-*p*$NO_2$ prepared with [Dz-*p*$NO_2$] = 12.8 μM, (b) lf-SWCNTs-*p*$NO_2$ prepared with [Dz-*p*$NO_2$] = 25.6 μM, (c) lf-SWCNTs-*o*P prepared with [Dz-*o*P] = 3.2 μM and (d) lf-SWCNTs-*o*P prepared with [Dz-*o*P] = 6.4 μM before (upper panels) and after (lower panels) CNT micelle polymerization. Measurements were performed in $D_2O$.

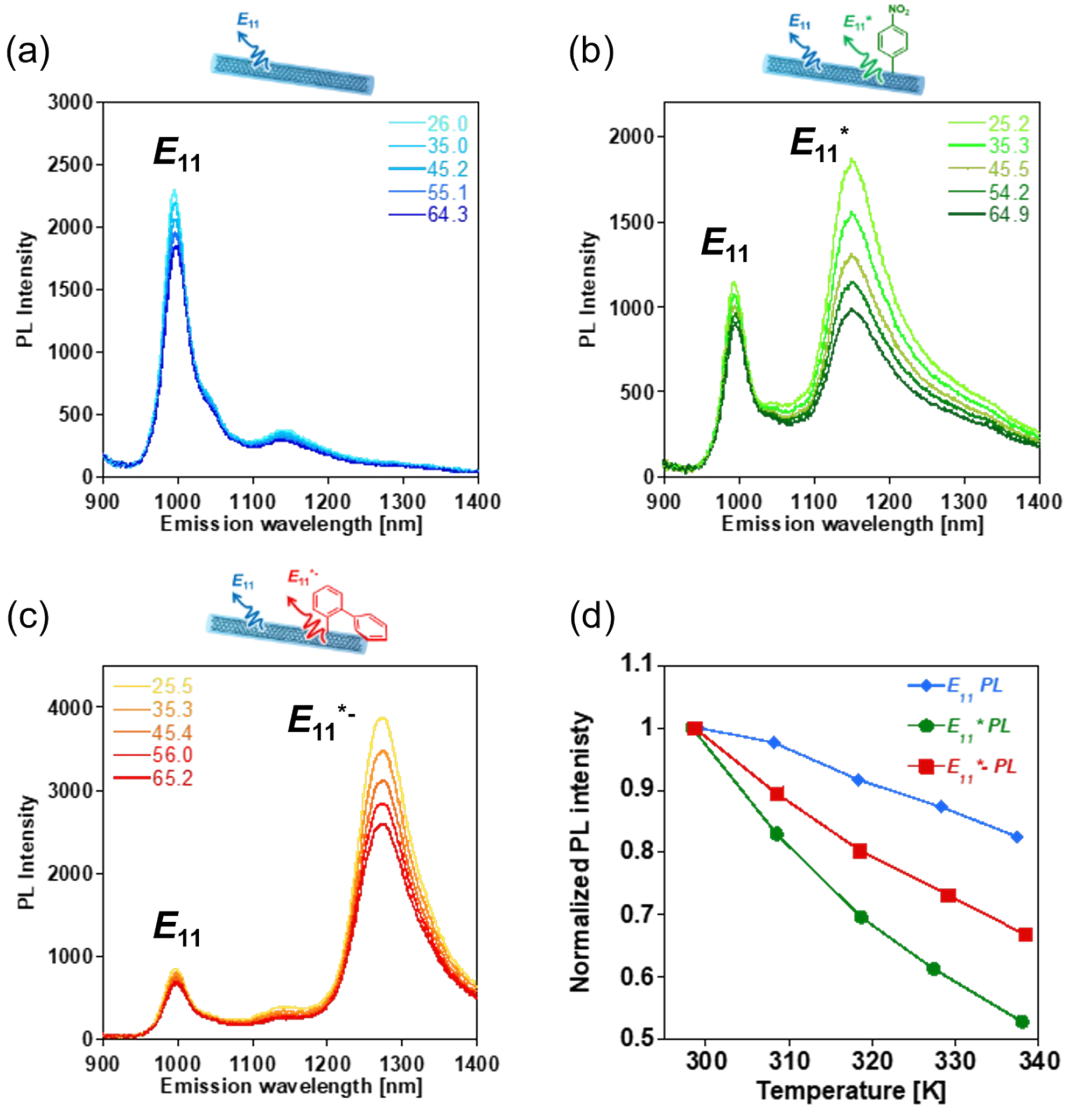


**Fig. S10** PL spectra (excitation: 570 nm) of (a) gel-coated SWCNTs, (b) gel-coated lf-SWCNTs-*p*$NO_2$ and (c) gel-coated lf-SWCNTs-*o*P measured at different temperature. (d) Plots of normalized PL intensity at different temperature of $E_{11}$ PL of gel-coated SWCNTs (blue), $E_{11}^*$ PL of gel-coated lf-SWCNTs-*p*$NO_2$ (green) and $E_{11}^{*-}$ PL of gel-coated lf-SWCNTs-*o*P (red).

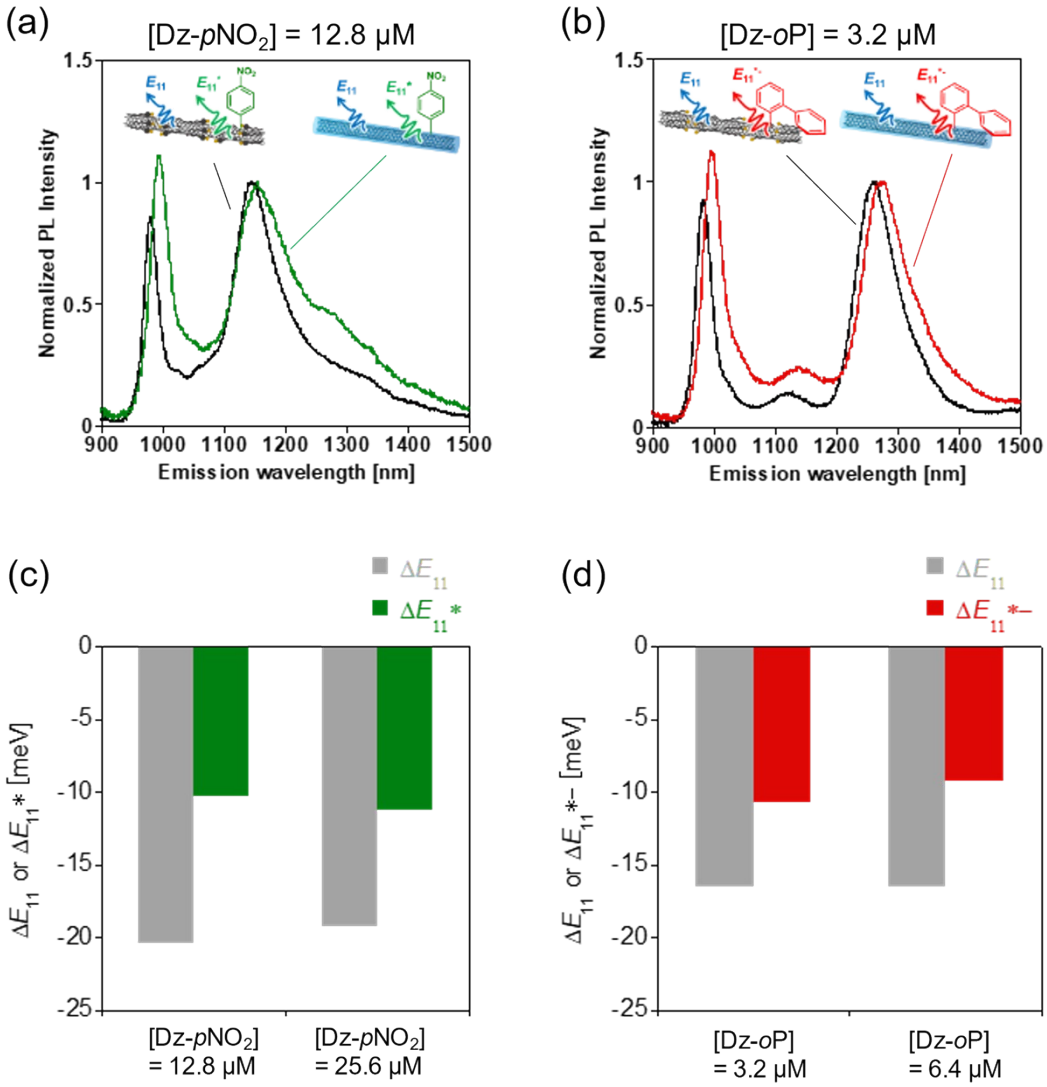


**Fig. S11** (a) PL spectra (excitation: 570 nm) of SDBS-dispersed lf-SWCNT-*p*$NO_2$ in (black) and gel-coated lf-SWCNT-*p*$NO_2$ (green), both of which were prepared with [Dz-*p*$NO_2$] = 12.8 μM in $D_2O$. (b) PL spectra (excitation: 570 nm) of SDS-dispersed lf-SWCNT-*o*P (black) and gel-coated lf-SWCNT-*o*P, both of which were prepared with [Dz-*o*P] = 3.2 μM in $D_2O$. (c) Energy shift values of $E_{11}$ and $E_{11}^*$ PL after gel coating of lf-SWCNTs-*p*$NO_2$ synthesized at different [Dz-*p*$NO_2$]. (d) Energy shift values of $E_{11}$ and $E_{11}^{*-}$ PL due to gel coating of lf-SWCNTs-*o*P synthesized at different [Dz-*o*P].

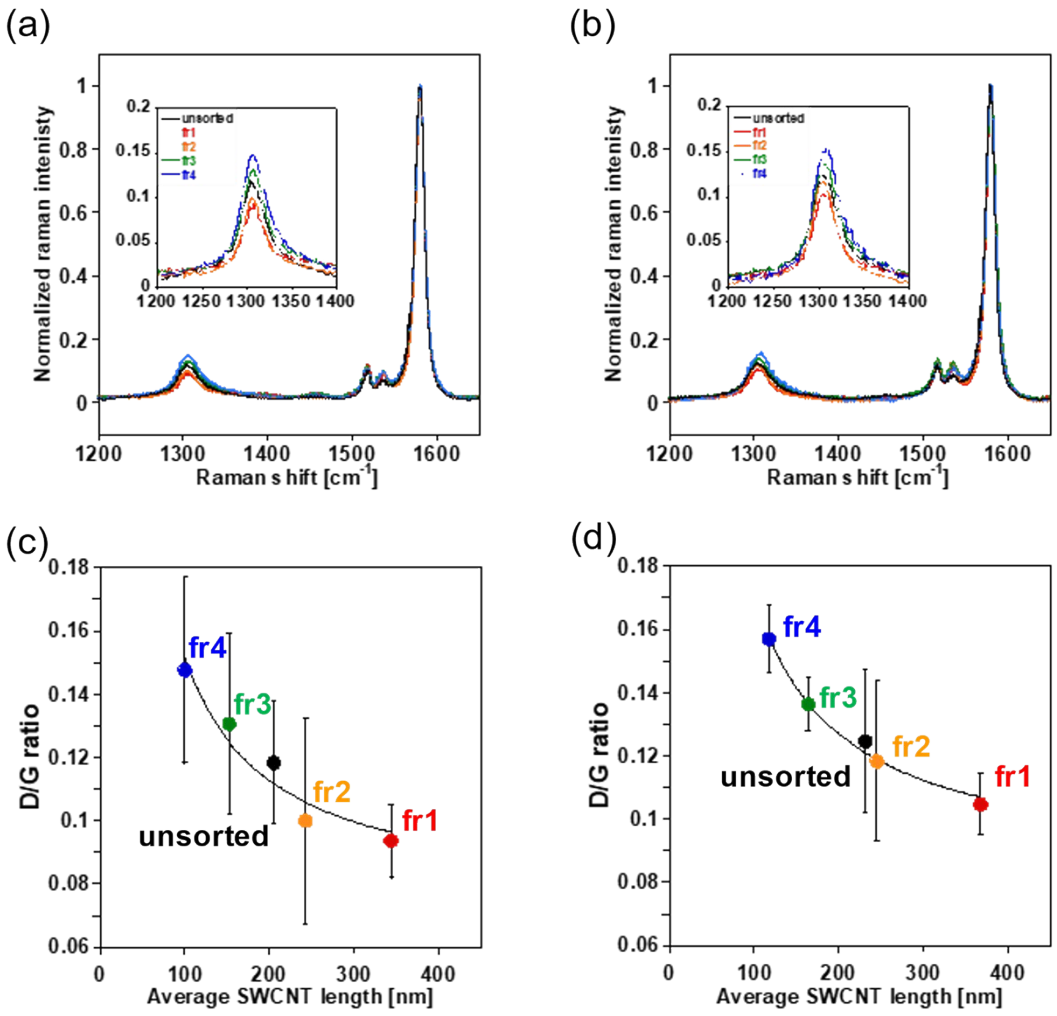


**Fig. S12** (a, b) Raman spectra and (c, d) D/G ratio of unsorted and length sorted gel-coated lf-SWCNTs-*p*$NO_2$ (a, c) and gel-coated lf-SWCNTs-*o*P (b, d). The D/G ratio was fitted as a function of the inverse of the average SWCNT length (~1/L). Error bars mean standard deviation calculated from five different measurement points.

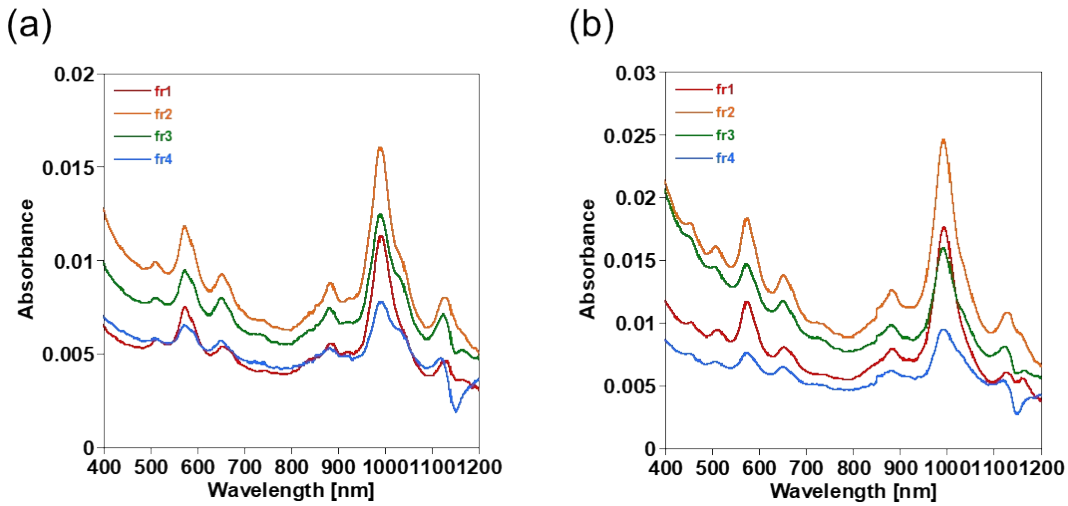


**Fig. S13** Absorption spectra of fr1 (red), fr2 (orange), fr3 (green) and fr4 (blue) of (a) gel-coated lf-SWCNTs-*p*$NO_2$ and (b) gel-coated lf-SWCNTs-*o*P.

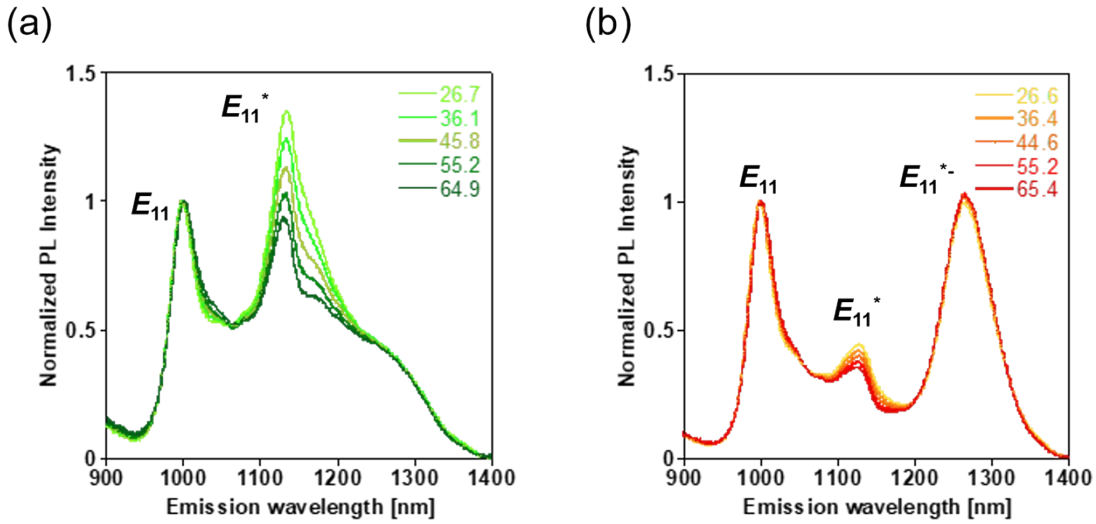


**Fig. S14** PL spectra (excitation: 570 nm) of unsorted (a) gel-coated lf-SWCNTs-*p*$NO_2$ and (b) gel-coated lf-SWCNTs-*o*P in $H_2O$ measured at different temperature.

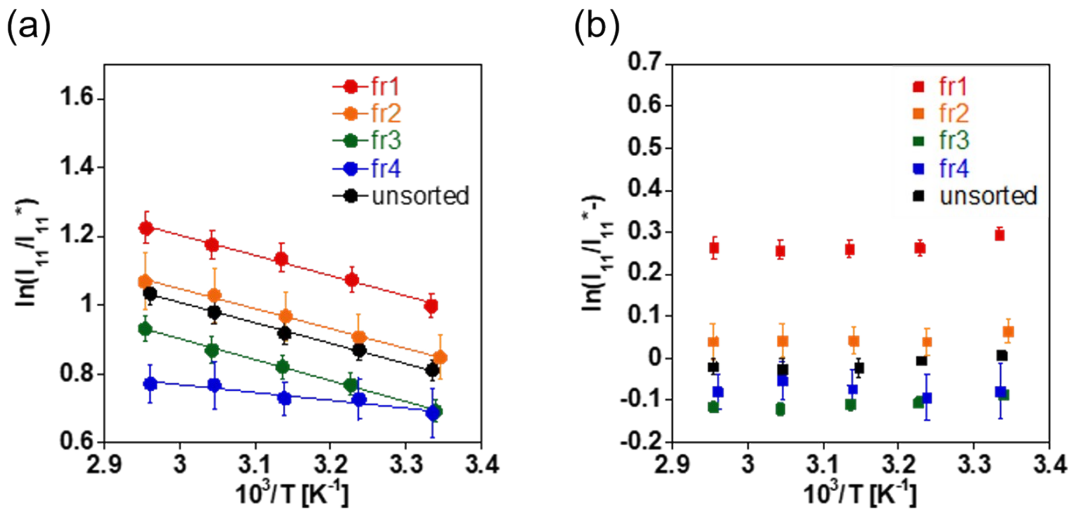


**Fig. S15** The Van't Hoff plot of unsorted and length sorted gel-coated lf-SWCNTs-*o*P $E_{11}^{*}$ PL (a) and $E_{11}^{*}$- PL (b) in $H_2O$. Error bars mean the error estimated during peak deconvolution.